Electronic Supplementary Material (ESI) for Journal of Materials Chemistry B.

Supporting Information

Dual Drug-Paired Polyprodrug Nanotheranostics Reverse Multidrug Resistant Cancers via Mild Photothermal-Cocktail Chemotherapy

Chang Du[1], Yue Ding[1], Jiwen Qian[1], Rong Zhang[2,*], Chang-Ming Dong[1,*]

[1]School of Chemistry and Chemical Engineering, Shanghai Key Laboratory of Electrical Insulation and Thermal Aging, Shanghai Jiao Tong University, Shanghai 200240, P. R. China

[2]Department of Obstetrics and Gynecology, Shanghai Fengxian Central Hospital, Southern Medical University, Shanghai 201499, P. R. China

E-mail address: cmdong@sjtu.edu.cn (C. M. Dong); rongzhang@163.com (R. Zhang)

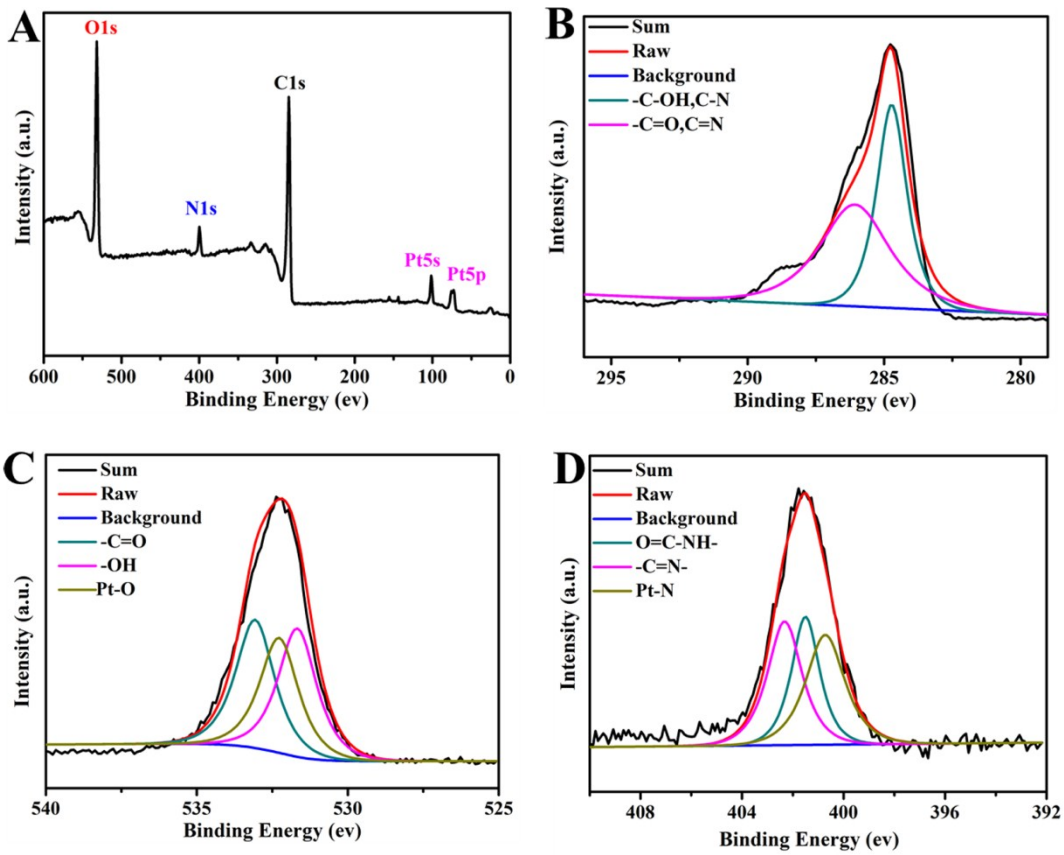

Fig. S1 XPS (A) and the related spectra of C1s (B), O1s (C), and N1s (D) of $PDCN_{25}$-CDDP.

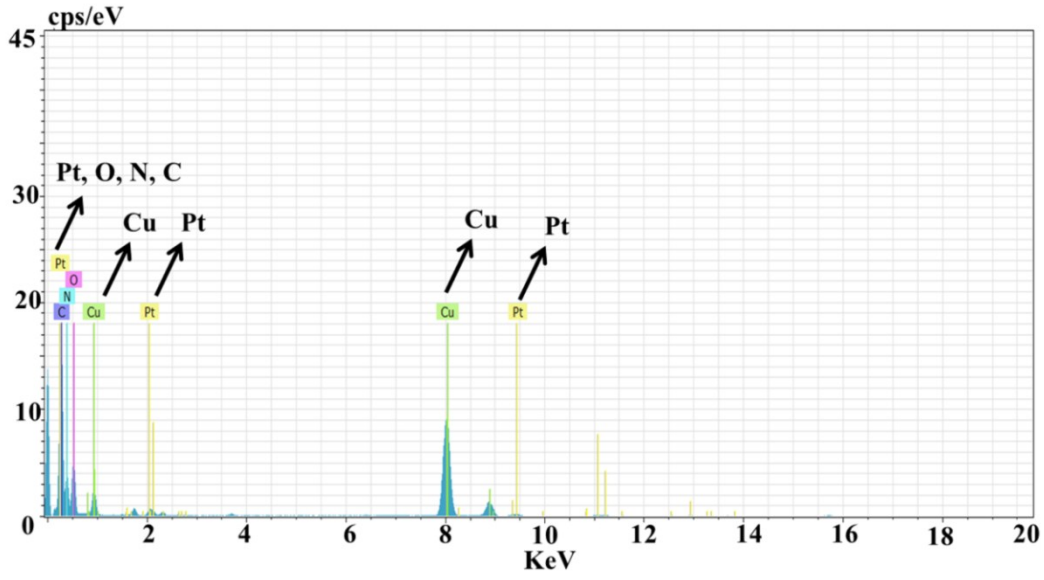

Fig. S2 The EDX profile of $PDCN_{25}$-CDDP.

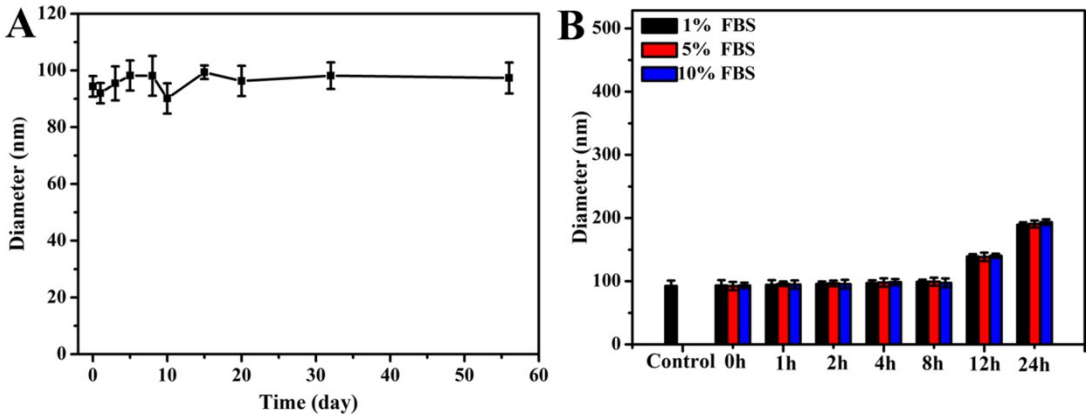

Fig. S3 The dependence of the $PDCN_{25}$-CDDP size on incubation time in PBS at 4 °C (A) or in the presence of FBS at 37 °C (B) (n = 3).

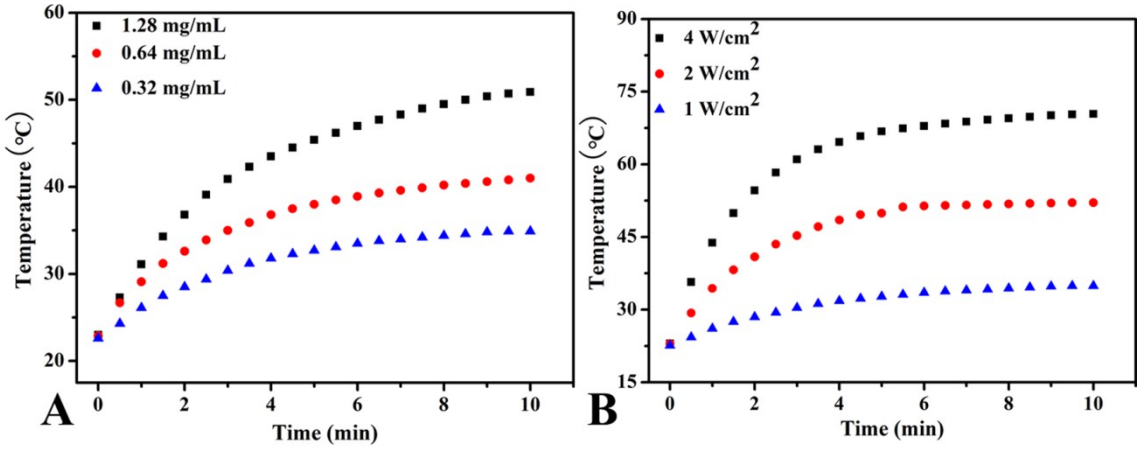

Fig. S4. (A) Heating curves of $PDCN_{25}$-CDDP with different concentrations as a function of irradiation time upon the NIR irradiation (808 nm, 1 W/cm^2, 10 min) or (B) the ones with different power intensities.

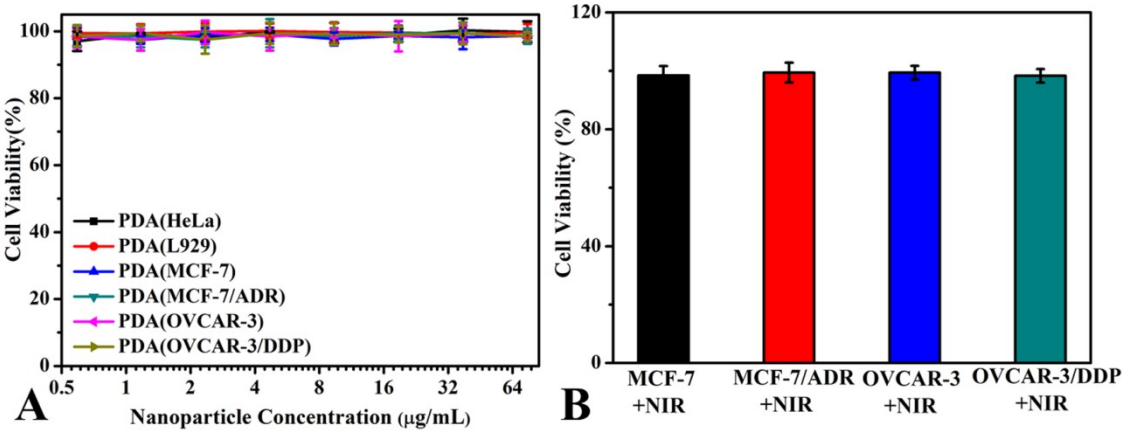

Fig. S5 The cytotoxicity of PDA (A) or mild NIR irradiation (B) on HeLa, L929, MCF-7， MCF-7/ADR, OVCAR-3, and OVCAR-3/DDP cell lines. All samples were tested in six replicates (n = 6).

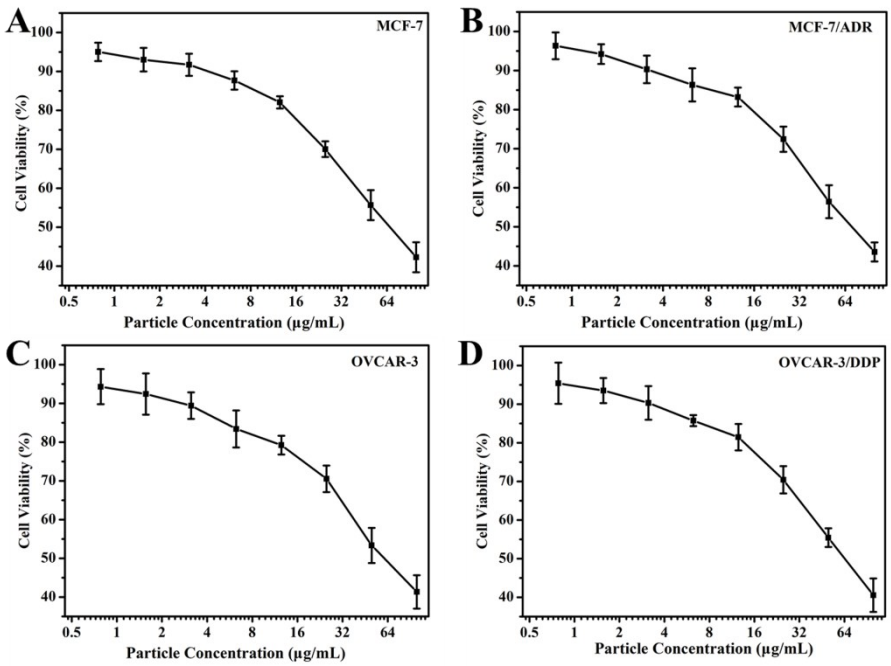

Fig. S6 Photothermal cytotoxicity of PDA incubated with MCF-7 (A) or MCF-7/ADR (B) or OVCAR-3 (C) or OVCAR-3/DDP (D) upon mild NIR irradiation. All samples were tested in six replicates (n = 6).

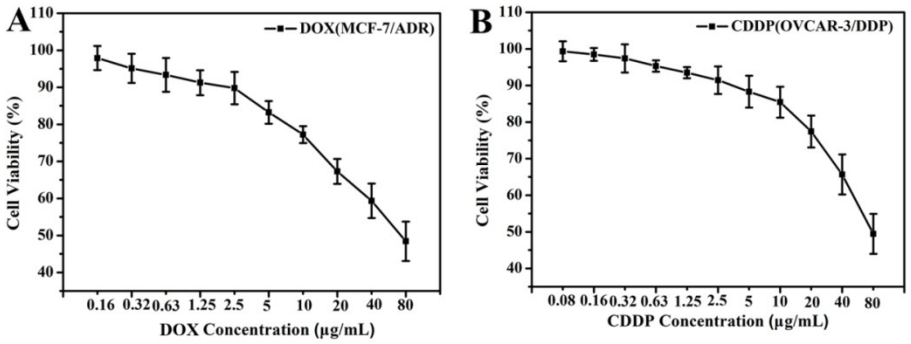

Fig. S7 Cytotoxicity of DOX or CDDP incubated with MCF-7/ADR (A) or OVCAR-3/DDP (B). All drug concentrations were tested in six replicates (n = 6).

Both MCF-7/ADR and OVCAR-3/DDP obviously produced multidrug resistance on free DOX and CDDP compared to MCF-7 and OVCAR-3, and the IC_{50} values of DOX and CDDP were calculated to be 73.01 and 89.60 μg/mL for MCF-7/ADR and OVCAR-3/DDP, respectively.

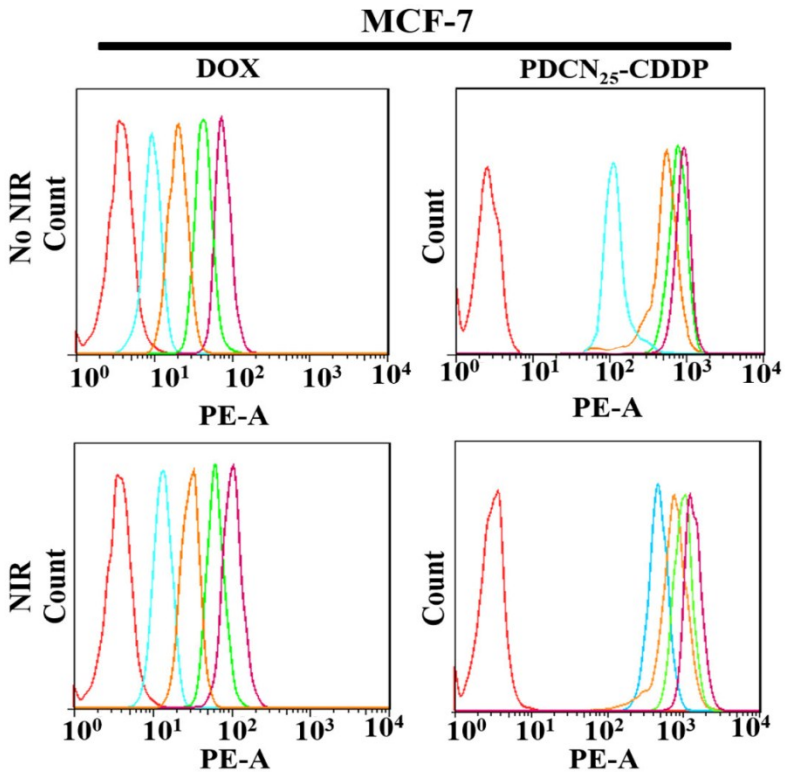

Fig. S8 Flow cytometry histograms of MCF-7 incubated with DOX or $PDCN_{25}$-CDDP with/without NIR irradiation for different times (red, control; blue, 0.5 h; orange, 1 h; green, 2h; purple, 4 h).

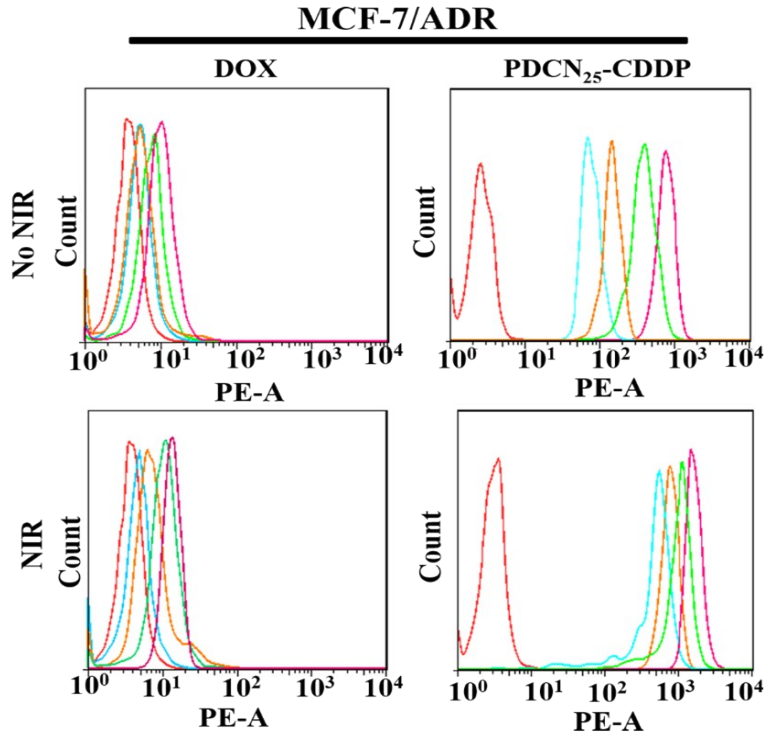

Fig. S9 Flow cytometry histograms of MCF-7/ADR incubated with DOX or $PDCN_{25}$-CDDP with/without NIR irradiation for different times (red, control; blue, 0.5 h; orange, 1 h; green, 2h; purple, 4 h).

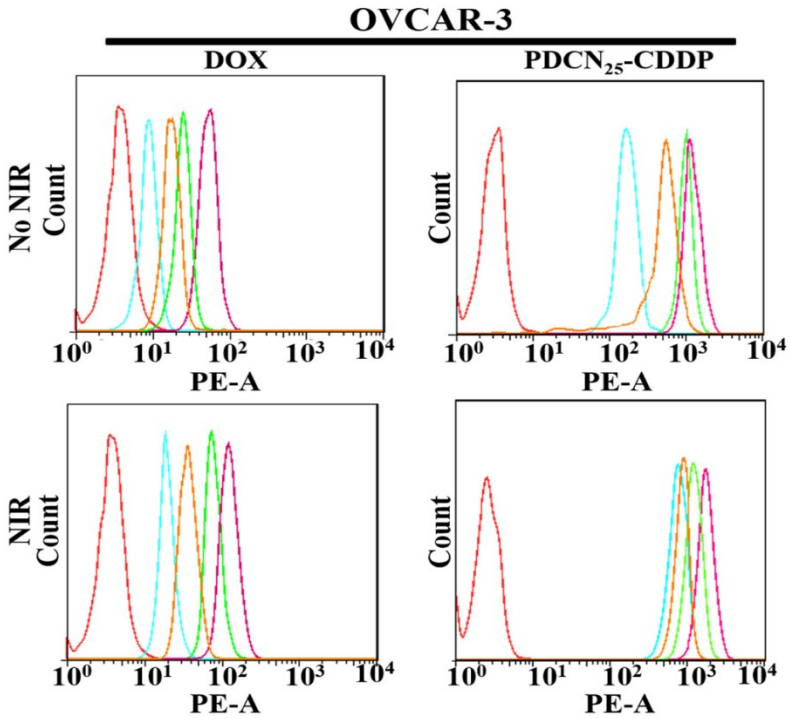

Fig. S10 Flow cytometry histograms of OVCAR-3 incubated with DOX or $PDCN_{25}$-CDDP with/without NIR irradiation for different times (red, control; blue, 0.5 h; orange, 1 h; green, 2h; purple, 4 h).

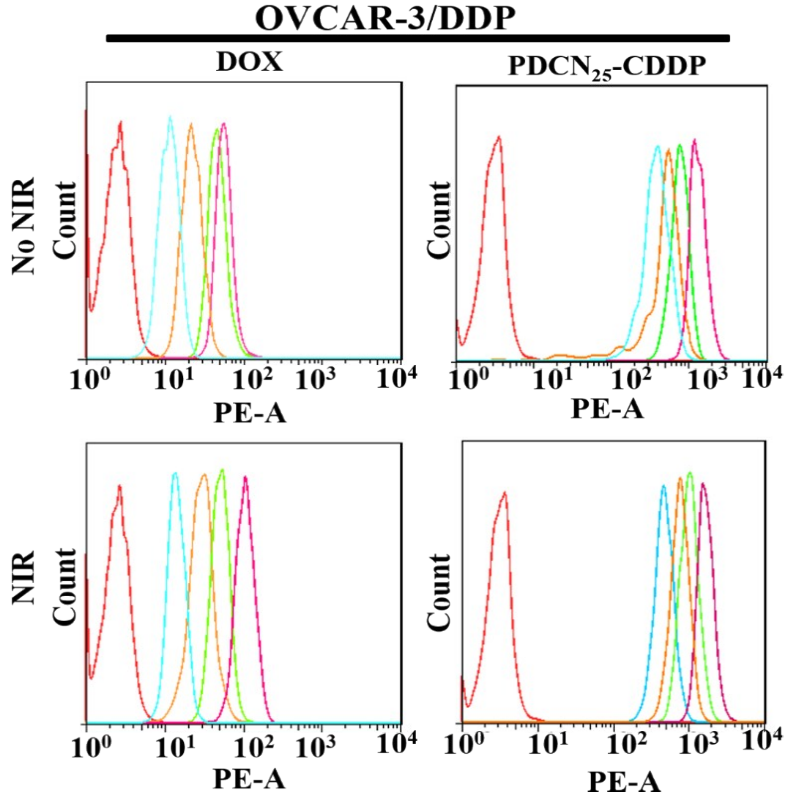

Fig. S11 Flow cytometry histograms of OVCAR-3/DDP incubated with DOX or $PDCN_{25}$-CDDP with/without NIR irradiation for different times (red, control; blue, 0.5 h; orange, 1 h; green, 2h; purple, 4 h).

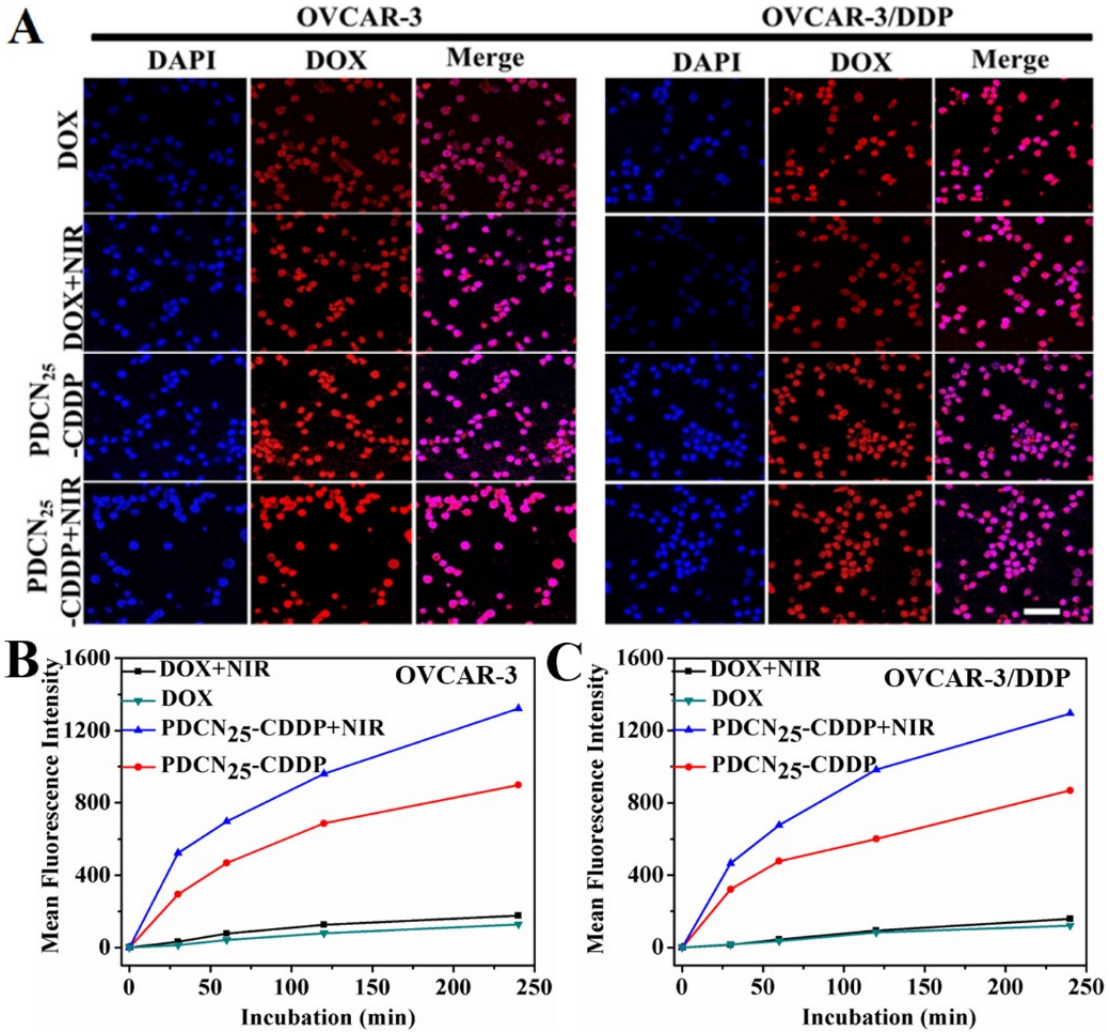

Fig. S12 (A) CLSM images and (B, C) the time-dependent fluorescence intensity of OVCAR-3 and OVCAR-3/DDP incubated with free DOX or $PDCN_{25}$-CDDP with/without NIR irradiation. The scale bar represents 20 μm.

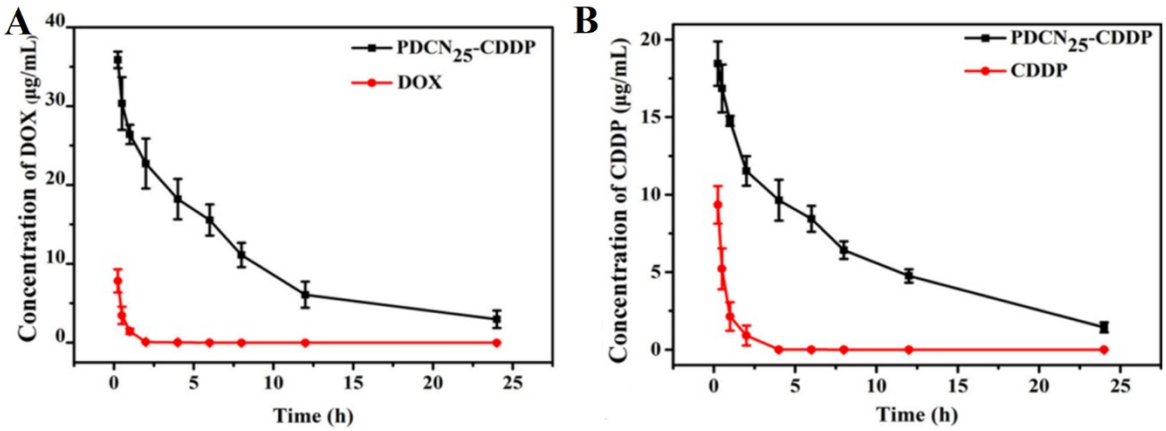

Fig. S13 (A, B) In vivo pharmacokinetics of $PDCN_{25}$-CDDP, DOX, and CDDP (n = 4).

The elimination half-life (t1/2β) of DOX and CDDP in $PDCN_{25}$-CDDP was (5.26 ± 1.09 h) and (8.10 ± 1.05 h) higher than that of free DOX (0.94 ± 0.10 h) and free CDDP (1.45 ± 0.36 h). The area under the curve (AUC) for DOX and CDDP in $PDCN_{25}$-CDDP was (237.25 ± 32.45 mg.h/L) and (139.03 ± 18.45 mg.h/L) much higher than that for free DOX (3.59 ± 0.56 mg.h/L) and free CDDP (6.11 ± 0.52 mg.h/L). In short, these results illustrated that the dual drug paired polyprodrug nanoparticle of $PDCN_{25}$-CDDP could prolong the blood circulation times of free DOX and CDDP pair due to their nanoscale and prodrug characteristics, enabling it physiologically stable for achieving efficient CCT in vivo.

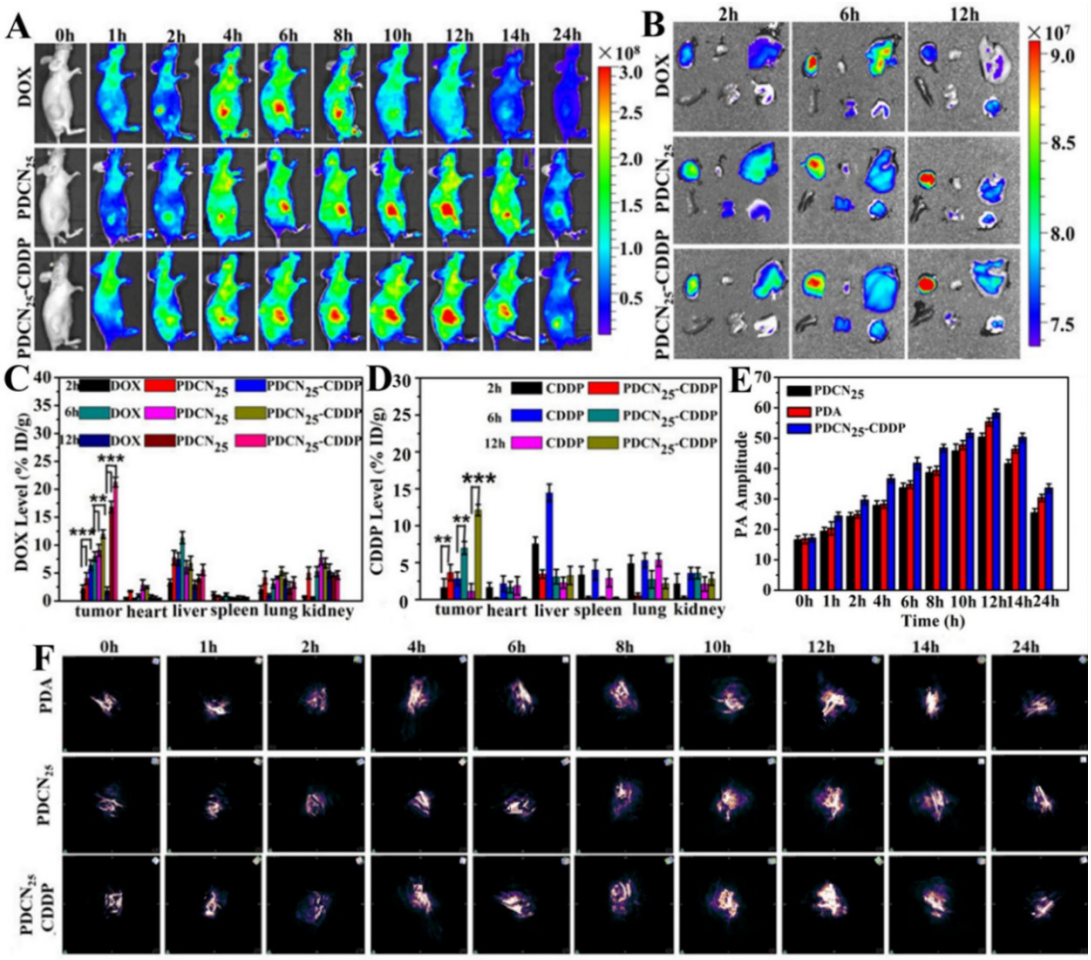

Fig. S14 (A) In vivo fluorescent imaging of the OVCAR-3/DDP tumor-bearing mice after intravenous injection of DOX or $PDCN_{25}$ or $PDCN_{25}$-CDDP; (B) ex vivo imaging of the major organs and the tumors; biodistributions of DOX (C, 5 mg/kg) and CDDP (D, 2.5 mg/kg) in different tissues. **P < 0.005, ***P < 0.001; (E) the PA signal intensity and (F) 3D imaging of tumor at different time intervals (n = 3).

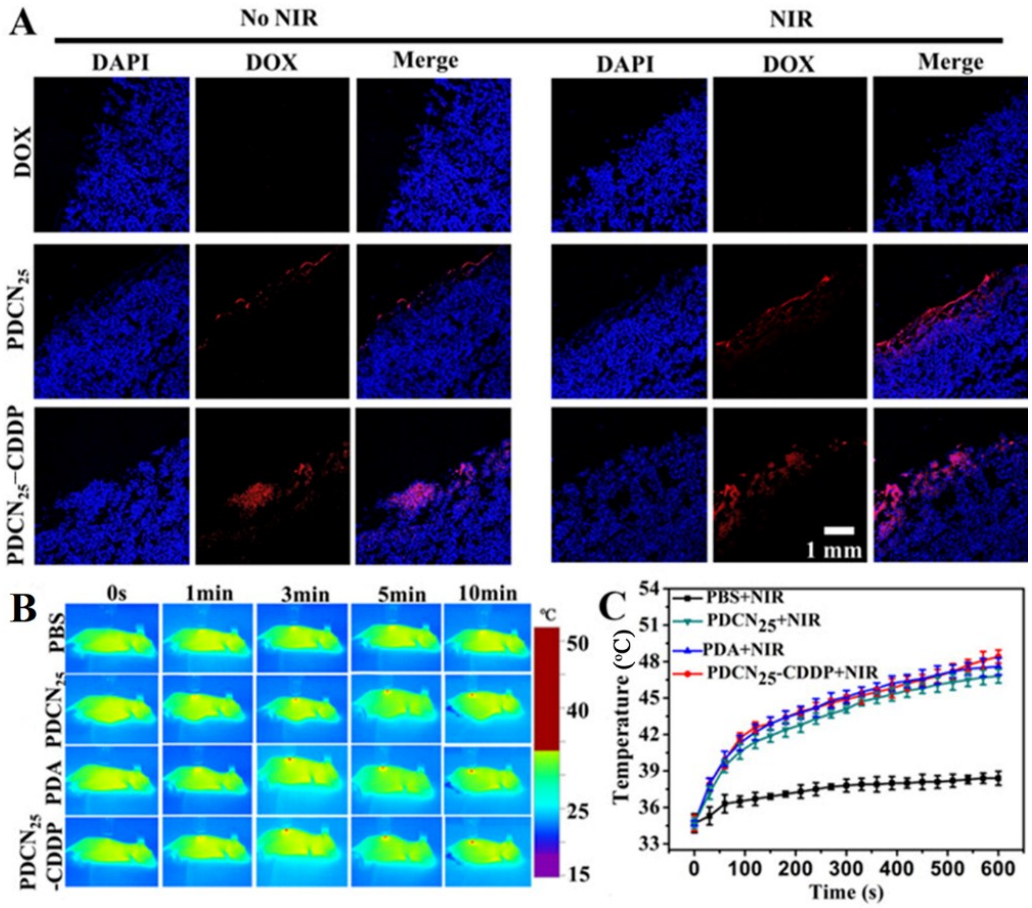

Fig. S15 (A) CLSM images of frozen tumor sections for examining ex vivo MCF-7/ADR tumor penetration; (B) the photothermal imaging of OVCAR-3/DDP tumor-bearing nude mice; and (C) the temperature evolution curve of the OVCAR-3/DDP tumor site over irradiation time (n = 4).

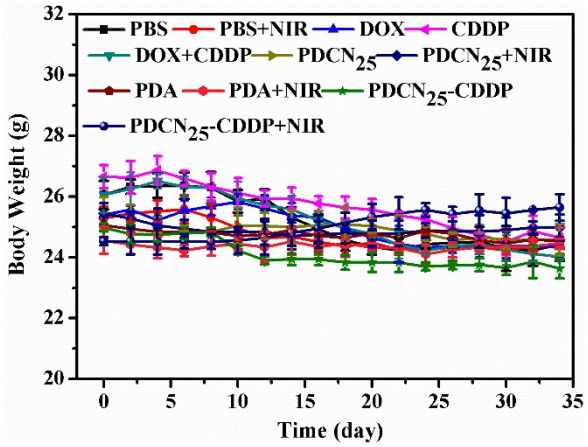

Fig. S16 The dependence of body weight of the MCF-7/ADR mice on time after various treatments (n = 4).

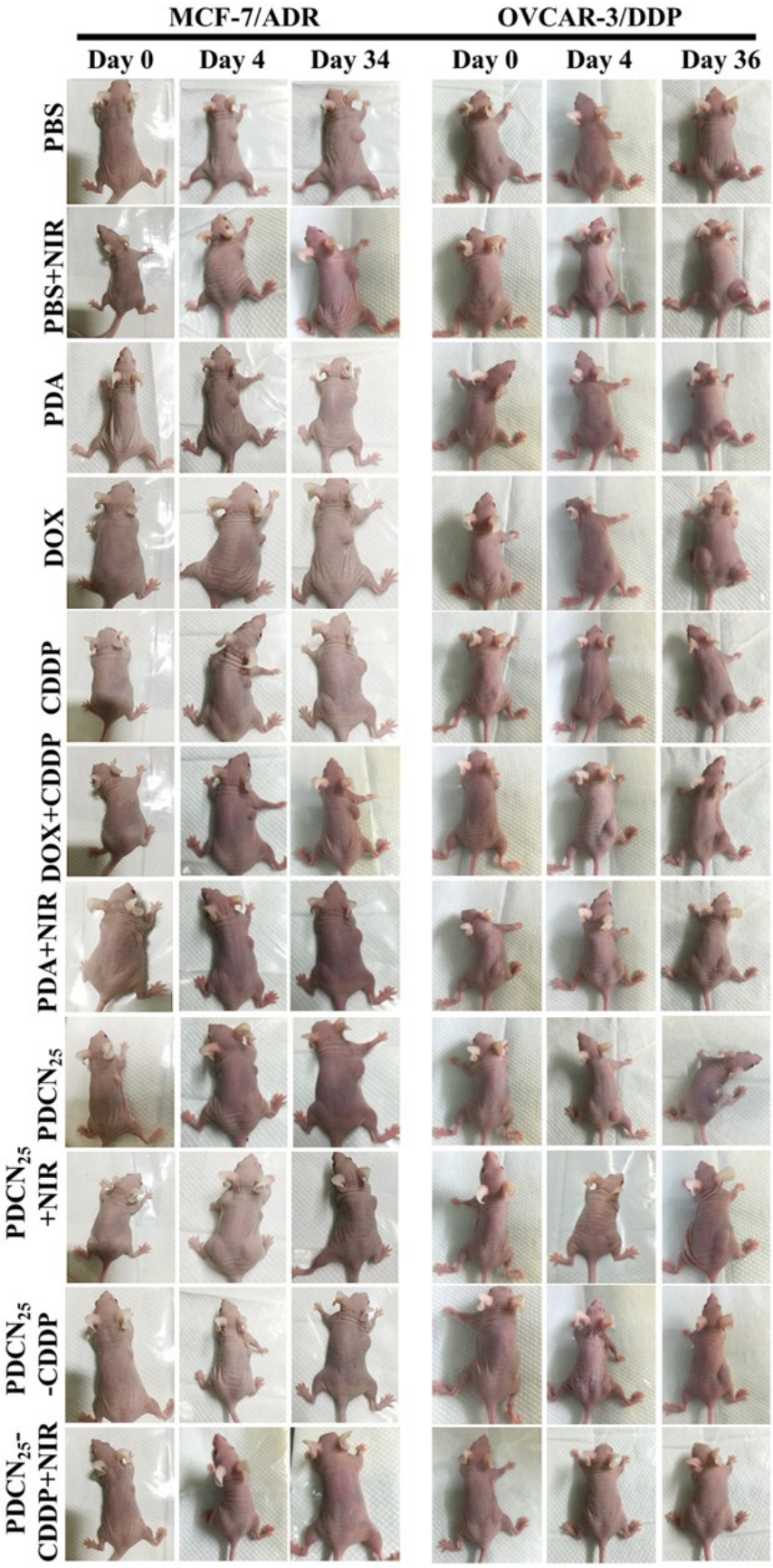

Fig. S17 The photographs of the small MCF-7/ADR and OVCAR-3/DDP tumor-bearing mice (60–80 mm^3) with various treatments.

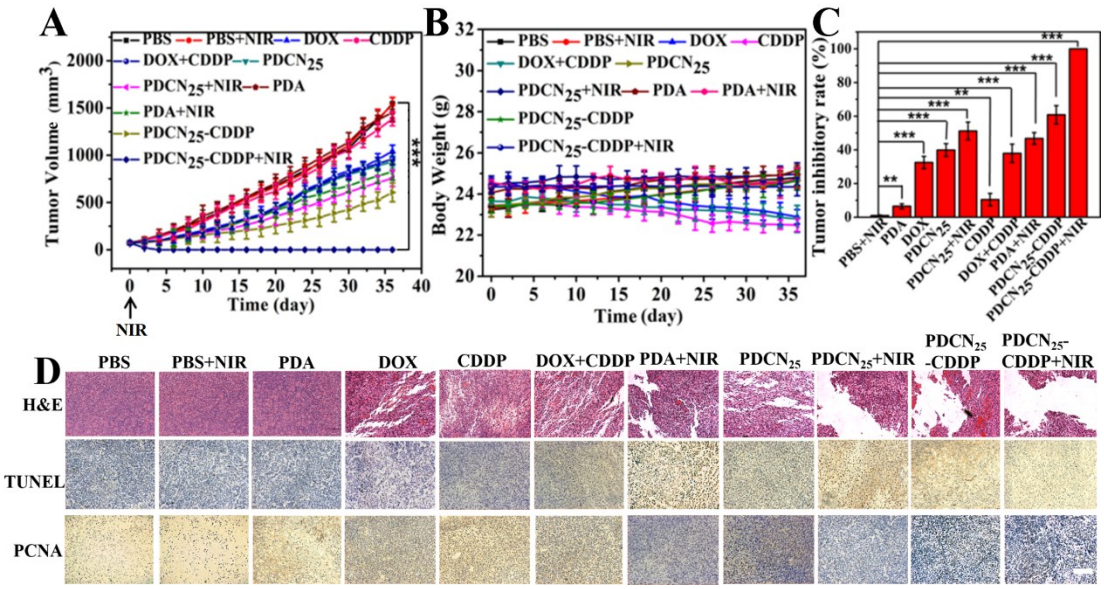

Fig. S18 (A) The tumor volume and (C) tumor inhibitory rate of small OVCAR-3/DDP tumor model (60–80 mm^3) over time after various treatments (the arrow denotes one intravenous injection), **P < 0.005, ***P < 0.001 (n = 4); (B) the dependence of body weight of the OVCAR-3/DDP mice on time after various treatments; H&E stained images, TUNEL, and PCNA (D) of the dissected tumors after 36 days treatment and the healed tissue for the $PDCN_{25}$-CDDP+NIR group, and the scale bar represents 150 μm.

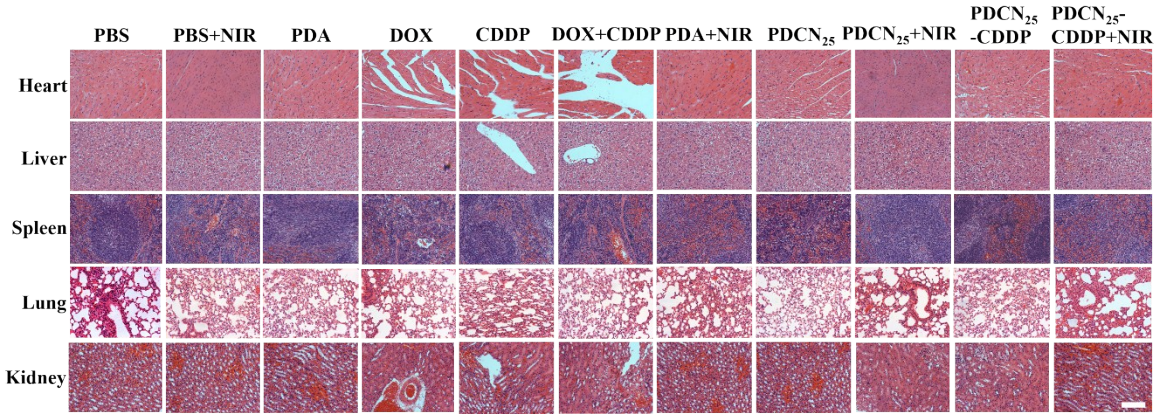

Fig. S19 H&E staining images of the tissue sections from the main organs including liver, kidneys, spleen, lung, and heart from the MCF-7/ADR tumor-bearing nude mice with various treatments and the scale bar represents 150 μm.

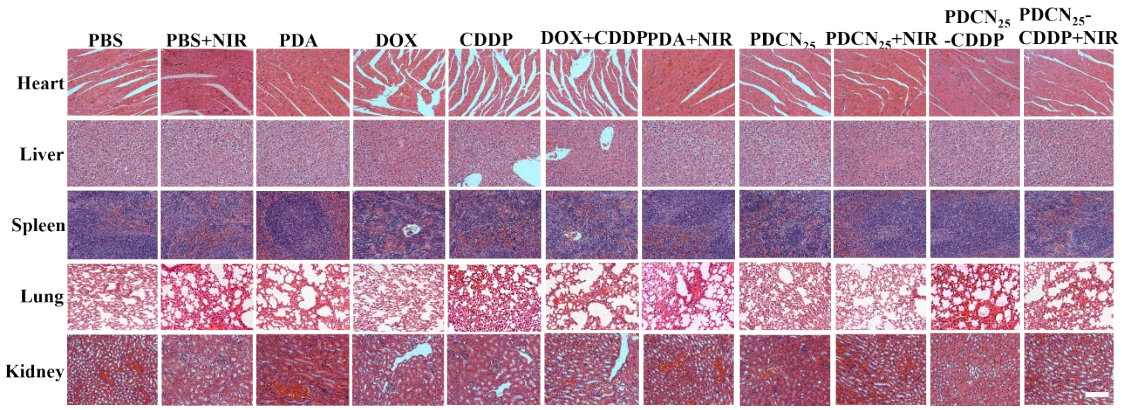

Fig. S20 H&E staining images of the tissue sections from the main organs including liver, kidneys, spleen, lung, and heart from the OVCAR-3/DDP tumor-bearing nude mice with various treatments and the scale bar represents 150 μm.

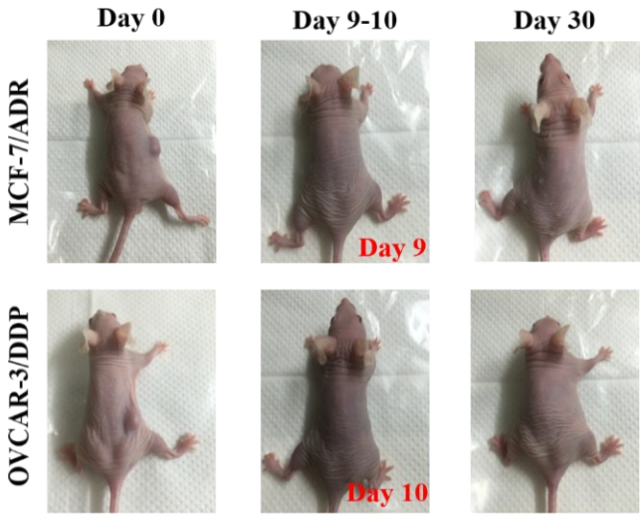

Fig. S21 The photographs of the big MCF-7/ADR and OVCAR-3/DDP tumor-bearing mice (240–270 mm^3) after the PT-CCT treatment.